

GAN-Based Interactive Reinforcement Learning from Demonstration and Human Evaluative Feedback

Jie Huang^{1*}, Rongshun Juan^{1*}, Randy Gomez², Keisuke Nakamura², Qixin Sha¹, Bo He¹, Guangliang Li^{1**}

Abstract—Deep reinforcement learning (DRL) has achieved great successes in many simulated tasks. The sample inefficiency problem makes applying traditional DRL methods to real-world robots a great challenge. Generative Adversarial Imitation Learning (GAIL) — a general model-free imitation learning method, allows robots to directly learn policies from expert trajectories in large environments. However, GAIL shares the limitation of other imitation learning methods that they can seldom surpass the performance of demonstrations. In this paper, to address the limit of GAIL, we propose GAN-Based Interactive Reinforcement Learning (GAIRL) from demonstration and human evaluative feedback by combining the advantages of GAIL and interactive reinforcement learning. We tested our proposed method in six physics-based control tasks, ranging from simple low-dimensional control tasks — Cart Pole and Mountain Car, to difficult high-dimensional tasks — Inverted Double Pendulum, Lunar Lander, Hopper and HalfCheetah. Our results suggest that with both optimal and suboptimal demonstrations, a GAIRL agent can always learn a more stable policy with optimal or close to optimal performance, while the performance of the GAIL agent is upper bounded by the performance of demonstrations or even worse than it. In addition, our results indicate the reason that GAIRL is superior over GAIL is the complementary effect of demonstrations and human evaluative feedback.

I. INTRODUCTION

REINFORCEMENT learning (RL) attempts to solve the challenge of building a robot that learns an optimal policy through interaction with the physical world via trial and error [1], [2]. With recent advances in deep neural network, deep reinforcement learning (DRL) — a combination of deep learning and RL, has achieved great successes in many simulated tasks, ranging from games [3], [4], [5] to complex locomotion behaviors [6], [7] and robotic manipulators [8]. However, shared by RL, DRL is sample inefficient and slow to converge because of the scarce reward signals [9]. It is difficult or even unpractical to design an efficient reward function for each task, which makes applying traditional DRL methods to real-world robots a great challenge [10].

Since most robots will operate in human inhabited environments, the ability to interact and learn from human users will be key to their success [11]. Many approaches for robot learning from interaction with a human user have

been proposed. The interactive feedback that the human user provides during such interaction can take many forms, e.g., demonstrations, preferences, evaluative feedback, etc. Among them, imitation learning from demonstrations was proposed and often leads to faster learning than learning from reward signals [12], [13], [14], [15], [16], [17], [18]. In addition, it would be much easier to demonstrate behaviors than designing reward functions for robots to learn, though reward functions are commonly used to specify the objective of robots.

The simplest approach in this setting is behavioral cloning (BC) [12], in which the goal is to learn the mapping from states to optimal actions as a supervised learning problem. However, BC needs large amounts of data to learn and cannot generalize to unseen states, which is commonly used to initialize policies for RL [19], [20]. Another approach is inverse reinforcement learning (inverse RL), which learns a policy via RL, using a cost function extracted from expert trajectories [13]. Because of the assumption of expert optimality as prior on the space of policies, inverse RL can allow the learner to generalize expert behavior to unseen states more effectively [21]. However, many of the proposed inverse RL algorithms need a model to solve a sequence of planning or reinforcement learning problems in an inner loop [22], which is extremely expensive to run and limits their use in large and complex tasks. Moreover, their agents' performance might significantly degrade if the planning problems are not solved to optimality [21], [23]. Therefore, by drawing an analogy between imitation learning and generative adversarial networks (GANs) [24], Ho et al. proposed Generative Adversarial Imitation Learning (GAIL) — a general model-free framework for directly learning policies from the expert trajectories [22], and extended inverse RL to large environments. However, GAIL shares the limitation of the other imitation learning methods that they can seldom surpass the performance of demonstrations. In many tasks, demonstrations are not always optimal or the optimal demonstrations are hard to obtain practically. If the behavior of the demonstrator is suboptimal or far from optimal, the same will hold for GAIL. Moreover, the performance of policies trained through adversarial methods still falls short of those produced by manually designed reward functions, when such reward functions are available [19], [25], [26].

Fortunately, an agent via interactive reinforcement learning (interactive RL) from human evaluative feedback can generally surpass a trainer's performance in the task [27], [11]. Based on reward shaping [28] in traditional RL, interactive RL from human evaluative feedback allows even non-technical people

¹College of Information Science and Engineering, Ocean University of China, {{bhe, guangliangli}@ouc.edu.cn

²Honda Research Institute Japan Co., Ltd, Wako, Japan. {r.gomez, keisuke}@jp.honda-ri.com

* Contributing equally

** Corresponding author

to train robots by evaluating their behaviors [29]. Hence, in this paper, we propose a model-free framework — GAN-Based Interactive Reinforcement Learning (GAIRL), which combines the advantages of GAIL and interactive RL from human evaluative feedback. We hypothesize agents learn via GAIRL can outperform the demonstration performance and acquire an optimal policy disregarding the quality of demonstrations. We tested our method in six physics-based control tasks from the classic RL literature, ranging from simple low-dimensional control tasks — Cart Pole and Mountain Car, to difficult high-dimensional tasks — Inverted Double Pendulum, Lunar Lander, Hopper and HalfCheetah. Our results suggest that with both optimal and suboptimal demonstrations, a GAIRL agent can always learn a more stable policy with optimal or close to optimal performance, while the performance of the GAIL agent is upper bounded by the performance of demonstrations or even worse than it. In addition, our results indicate the reason that GAIRL is superior over GAIL might be because of the complementary effect of demonstrations and human evaluative feedback.

II. RELATED WORK

This section surveys the most related work to our approach in terms of imitation learning via inverse reinforcement learning and interactive reinforcement learning.

A. Imitation Learning via Inverse Reinforcement Learning

The inverse RL problem is to learn a policy via RL, using a cost function extracted from expert trajectories that prioritizes entire trajectories over others [13]. As a result, inverse RL does not suffer from compounding error problems as behavioral cloning [12]. Moreover, because the assumption of expert optimality acts as prior on the space of policies, inverse RL can allow the learner to generalize expert behavior to unseen states more effectively [21].

In inverse RL, commonly, the reward function can be modeled via a linear combination of feature weights [14]. There are many inverse RL algorithms using this linear approximation for the reward function including apprenticeship learning [14], maximum entropy inverse RL [17], etc. While many existing methods for apprenticeship learning output policies that are “mixed”, i.e., randomized combinations of stationary policies, apprenticeship learning using linear programming (LP) produces stationary policies [15]. However, it takes too much time for LP solver in an inner loop and the performance can significantly degrade if the planning problems are not solved to optimality [23]. Based on a game-theoretic view of the problem, the game-theoretic apprenticeship learning is computationally faster, easier to implement, and even can be applied in the absence of an expert [16]. However, recovering the agent’s exact weights of linear approximation for the reward function is an ill-posed problem: multiple rewards can explain a single behavior [13]. Based on the principle of maximum entropy [30], D.Ziebart et al. [17] proposed maximum entropy inverse RL to resolve the ambiguity in choosing a distribution over decisions.

Most of above mentioned inverse RL methods need a model to solve a sequence of planning or reinforcement learning problems in an inner loop, which is extremely expensive to run and limit their use in large and complex tasks. Ho et al. [21] proposed an imitation learning method by exploiting to learn a class of cost functions via distinguishing the expert policy from all others. Taking further inspiration from the success of nonlinear cost function classes in inverse RL [31], Ho et al. [22] proposed GAIL by drawing an analogy between imitation learning and generative adversarial networks (GANs). GAIL is a general model-free framework for directly learning policies from the expert trajectories and extends inverse RL to large environments. Instead of learning from demonstrations supplied in the first-person, third-person imitation learning [32] improves upon GAIL by recovering a domain-agnostic representation of the agent’s observations. Generative adversarial imitation from observation [33] learns directly from state-only demonstrations without having access to the demonstrator’s actions by recovering the state-transition cost function of the expert.

However, GAIL inherits the problems of GANs, including possible training instability such as vanishing and exploding gradients, which stands out when the given expert demonstrations are not optimal [34]. By introducing a new type of variational autoencoder on demonstration trajectories, Wang et al. [35] increased the robustness of GAIL and avoided its mode collapse. In addition, Peng et al. [25] effectively modulated the discriminator’s accuracy and maintain useful and informative gradients by enforcing a constraint on the mutual information between the observations and the discriminator’s internal representation. Instead of adversarial imitation learning, there are also many other methods integrating the preprocessed expert demonstrations into extensions of classic RL algorithms [36], [37], [38], [39]. Our work overcomes the limitation shared by imitation learning that it seldom surpasses the performance of demonstrations by allowing it to learn from both demonstration and human evaluative feedback.

B. Interactive Reinforcement Learning

Inspired by potential-based reward shaping [28], interactive RL is proposed to solve the sample efficiency problem in both RL and DRL, and allow an agent to learn from interaction with human at the same time. Specifically, an interactive RL agent can learn from non-experts in agent design and programming [29]. In interactive RL, a human trainer can evaluate the quality of an agent’s behavior and give feedback to improve its behavior. For example, Thomaz and Breazeal [40] implemented a tabular Q-learning [41] agent learning from environmental and human rewards. The TAMER agent learns from only human reward signal by directly modeling it [42]. To facilitate an agent to learn in tasks with high-dimensional state space, Warnell et al. proposed deep TAMER using deep neural network to approximate the reward function [27]. Loftin et al. [43] take human feedback as one kind of categorical feedback strategy for the agent to learn. The COACH algorithm learns by interpreting human reward signal as feedback to the current executing control policy of a robot

[44]. COACH was also extended to deep COACH using deep neural network as function approximator for the policy [45]. In addition, most related to our work, Li et al. proposed a method allowing an agent to learn from both human demonstration and evaluative feedback [11]. Our work differs by allowing an agent to learn in complex environment with a GAN-based model-free method.

III. BACKGROUND

We consider an agent within the Markov decision process (MDP) framework. An MDP can be represented with a tuple $M = \{S, A, P, \mathbb{R}, \gamma\}$. $\pi \in \Pi$ is a policy that takes an action $a \in A$ given a state $s \in S$. Successor states are derived from the dynamic model $P(s' | s, a)$. During the process, the agent will get a cost or reward $c(s, a)$ which is from a cost or reward function $C : S \times A \rightarrow \mathbb{R}$. \mathbb{R} denotes the extended real numbers $\mathbb{R} \cup \{+\infty\}$. $\mathbb{E}_\pi[c(s, a)] \triangleq \mathbb{E}[\sum_{t=0}^T \gamma^t c(s_t, a_t)]$ denotes an expectation of the discounted return along the trajectory generated by policy π , where γ is a discounted factor and $\gamma \in (0, 1]$. Similarly, \mathbb{E}_τ means an empirical expectation with respect to trajectory samples τ . We use π_E to refer to the expert policy and τ_E to refer to the expert trajectory samples.

A. Maximum Entropy Inverse RL

The first step of inverse RL is to learn a cost function based on the given expert demonstrations. The cost function is learned such that it is minimal for the trajectories demonstrated by the expert and maximal for every other policy [14]. Adding another constraint of choosing the policy with maximum entropy can solve the problem that many policies can lead to the same demonstrated trajectories. The general form of this framework can be expressed as:

$$\begin{aligned} \text{IRL}_\psi(\pi_E) = \arg \max_{c \in \mathbb{R}^{S \times A}} & -\psi(c) + (\min_{\pi \in \Pi} -H(\pi) + \\ & \mathbb{E}_\pi[c(s, a)] - \mathbb{E}_{\pi_E}[c(s, a)]), \end{aligned} \quad (1)$$

where $\psi(c) : \mathbb{R}^{S \times A} \rightarrow \mathbb{R}$ is a convex cost function regularizer, $H(\pi)$ is the entropy function of the policy π defined by $H(\pi) \triangleq \mathbb{E}_\pi[-\log \pi(a | s)]$. This step will output a desired cost function. Then the second step of maximum entropy inverse RL is an entropy-regularized RL step using the learned cost function, which can be defined as:

$$\text{RL}(c) = \arg \min_{\pi \in \Pi} -H(\pi) + \mathbb{E}_\pi[c(s, a)]. \quad (2)$$

The aim of the RL step is to find a policy minimizing the cost function and maximizing the entropy.

B. GAIL

Ho et al. [22] replaced the $\psi(c)$ in Eq.(1) with a new cost regularizer $\psi_{GA}(c)$, which penalizes slightly on cost functions that assign small costs to expert state-action pairs and penalizes heavily otherwise. Instead of running RL after IRL, GAIL directly learns the optimal policy in the way that brings the distribution of the state-action pairs of the agent as close as possible to that of the demonstrator. The circuitous

process summed up as Eq.(1) and Eq.(2) can be solved by finding a saddle point (π, D) of the expression:

$$-\lambda H(\pi) + \mathbb{E}_\pi[\log(D(s, a))] + \mathbb{E}_{\pi_E}[\log(1 - D(s, a))], \quad (3)$$

where a discriminator $D : S \times A \rightarrow (0, 1)$ is trained to distinguish expert transitions $(s, a) \sim \tau_E$ from agent transitions $(s, a) \sim \tau_{agent}$ expressed as minimizing $\mathbb{E}_\pi[\log(D(s, a))] + \mathbb{E}_{\pi_E}[\log(1 - D(s, a))]$. The agent is trained to “fool” the discriminator into thinking itself as the expert expressed as maximizing $\mathbb{E}_\pi[\log(D(s, a))]$. Taking $-\lambda H(\pi)$ out of Eq.(3), the loss function is analogous to that of GANs, which draws an analogy between imitation learning and GANs. In our work, we use the discriminator network as a cost function for further RL step. Originally, the algorithm used to optimize the policy is Trust Region Policy Optimization (TRPO) [46]. TRPO can prevent the policy from vibrating too much, as measured by KL divergence between the old policy and the new one averaged over the states in the trajectory samples, due to the noise in the policy gradient.

C. Interactive RL from Human Evaluative Feedback

Interactive RL was proposed to reduce the learning time of a RL agent based on reward shaping in traditional RL [28]. Interactive shaping, one of the classical interactive RL methods, allows an agent to learn to perform a task by interpreting human evaluative feedback as reward signals as in traditional RL [40], [42]. In interactive RL from human evaluative feedback, a human trainer can observe the agent’s behavior during the learning process and give evaluative feedback which will be used to update the agent’s policy. That is to say, when an agent takes an action a with respect to state s , the human trainer will provide evaluative feedback to imply the value of the selected action a . Then the agent will use this feedback as a reward to update the policy aiming to maximize cumulative rewards.

IV. PROPOSED APPROACH

To address the limit of GAIL that it seldom surpasses the performance of demonstrations, in this paper, we propose a model-free framework — GAN-Based Interactive Reinforcement Learning (GAIRL) by combining the advantages of GAIL and interactive RL from human evaluative feedback. GAIRL is expected to leverage human demonstrations and human evaluative feedback to improve the training of agents and outperform the demonstrator disregarding the quality of the demonstrations.

In GAIRL, besides the fixed cost function $c_{gail}(s, a)$ out of the discriminator as in GAIL, we introduce a human reward function into it as a new cost function, which can be expressed as:

$$c_{gairl}(s, a) = c_{gail}(s, a) + \alpha \mathbb{H}(s, a), \quad (4)$$

where $\mathbb{H}(s, a)$ is the human reward function approximated with a neural network (HRN), and α is a weight vector for balancing the cost function $c_{gail}(s, a)$ out of the discriminator in GAIL and the learned HRN. Specifically, we set

$$c_{gairl}(s, a) = -\log\left(\frac{e^{-D(s, a)}}{1 + e^{-D(s, a)}} + 10^{-8}\right). \quad (5)$$

In addition, Ho et al. [22] defined a policy's occupancy measure $\rho_\pi : S \times A \rightarrow \mathbb{R}$ as

$$\rho_\pi(s, a) = \pi(a|s) \sum_{t=0}^{\infty} \gamma^t P(s_t = s | \pi), \quad (6)$$

which means the unnormalized distribution of state-action pairs. They proved that

$$RL \circ IRL_{\psi_{GA}}(\pi_E) = \arg \min_{\pi \in \Pi} -\lambda H(\pi) + \psi_{GA}^*(\rho_\pi - \rho_{\pi_E}), \quad (7)$$

where ψ_{GA}^* is the convex conjugate of convex function ψ_{GA} . So we can try to solve $\arg \min_{\pi \in \Pi} -\lambda H(\pi) + \psi_{GA}^*(\rho_\pi - \rho_{\pi_E})$ directly instead of running RL after IRL as in other inverse RL methods. In our method, we use a new cost regularizer derived from ψ_{GA} , which can be expressed as

$$\psi_{gairl} \triangleq \begin{cases} \mathbb{E}_{\pi_E}[g(c_{gairl}(s, a))] & \text{if } c_{gairl} < 0 \\ +\infty & \text{otherwise,} \end{cases} \quad (8)$$

where

$$g(x) = \begin{cases} -x - \log(1 - e^x) & \text{if } x < 0 \\ +\infty & \text{otherwise.} \end{cases} \quad (9)$$

Its convex conjugate is shown as

$$\begin{aligned} \psi_{gairl}^*(\rho_\pi - \rho_{\pi_E}) &= \max_{D \in (0,1)^{S \times A}} \sum_{s,a} \rho_\pi(s, a) \log(D(s, a)) + \\ &\quad \rho_{\pi_E}(s, a) \log(1 - D(s, a)), \end{aligned} \quad (10)$$

where $D : S \times A \rightarrow (0, 1)$ is a discriminative classifier. Finally, our proposed approach can be summarized as solving

$$\begin{aligned} \min_{\pi \in \Pi} \psi_{gairl}^*(\rho_\pi - \rho_{\pi_E}) &= \min_{\pi \in \Pi} \max_{D \in (0,1)^{S \times A}} \mathbb{E}_\pi[\log(D(s, a))] + \\ &\quad \mathbb{E}_{\pi_E}[\log(1 - D(s, a))] - \lambda H(\pi) \end{aligned} \quad (11)$$

and then performing a RL step expressed as

$$RL(c_{gairl}) = \arg \min_{\pi \in \Pi} \mathbb{E}_\pi[c_{gairl}(s, a)]. \quad (12)$$

The proposed method is summarized in Algorithm 1, which contains two main steps. The first main step is the GAIL alike step, as shown in Algorithm 1 Part 1. Similar to GAIL, this step starts by sampling demonstrated trajectories from demonstrations and agent trajectories from the agent's current policy to perform the update on the discriminator. However, different from GAIL, in GAIRL, a human trainer, who might be non-expert in agent design or even in programming, can provide evaluative feedback by evaluating the agent's behavior according to her knowledge in the task. We use human evaluative feedback as labels of corresponding samples to train a human reward network (HRN) for predicting it. The standard mean square error is used as the loss function of HRN. Specifically, when the agent takes an action a in state s , a human trainer gives a reward R_h based on the evaluation of the state and action. Then we store the tuple $[s, a, R_h]$ in the replay buffer for HRN and randomly sample the tuple $[s, a, R_h]$ from the replay buffer to update HRN by minimizing the loss:

$$\mathcal{L}_{hrn} = \frac{1}{n} \sum_{i=0}^n (R_h - \mathbb{H}(s, a)), \quad (13)$$

Algorithm 1 Part 1

Input: Demonstrations \mathcal{E} , initialize agent's policy π_0 , discriminator D_0 and HRN \mathbb{H} , Replay Buffer $\mathcal{B}_1, \mathcal{B}_2$.

Output: Trained discriminator D and HRN \mathbb{H} , agent's policy π_i

- 1: Assign a human reward of $R_h = +1$ to all the state-action pairs $[s_d, a_d]$ from \mathcal{E}
 - 2: Store all the tuples $[s_d, a_d, +1]$ in $\mathcal{B}_1, \mathcal{B}_2$ respectively
 - 3: $i = 0$
 - 4: **repeat**
 - 5: Sample agent trajectories τ_i from π_i and demonstrated trajectories τ_E from \mathcal{E}
 - 6: **if** Receive human feedback R_h with respect to $[s, a]$ from τ_i **then** store $[s, a, R_h]$ in \mathcal{B}_1
 - 7: Randomly sample a batch of $[s, a, R_h]$ from \mathcal{B}_1
 - 8: Update \mathbb{H} using Rmsprop with loss \mathcal{L}_{hrn}
 - 9: **end if**
 - 10: Update D_i using Adam with loss $-(\mathbb{E}_{\tau_i}[\log(D_i(s, a))] + \mathbb{E}_{\tau_E}[\log(1 - D_i(s, a))])$
 - 11: Update π_i using TRPO with loss $-\lambda H(\pi) + \mathbb{E}_{\tau_i}[\log(D_{i+1}(s, a))]$
 - 12: $i = i + 1$
 - 13: **until** Meet Discriminator Requirements
 - 14: $D = D_i$
-

where $\mathbb{H}(s, a)$ is the estimated HRN. The human reward R_h is defined as below:

$$R_h = \begin{cases} +N & \text{agent reaches the goal} \\ +1 & \text{good action} \\ -1 & \text{bad action} \\ -N & \text{agent fails,} \end{cases} \quad (14)$$

where N is determined by different tasks (2 for Cart Pole, 6 for Mountain Car, 4 for Inverted Double Pendulum, 5 for Lunar Lander, Hopper and HalfCheetah). In addition, to ease the burden of the human trainer, we assign a human reward of $R_h = +1$ to all the state-action pairs $[s_d, a_d]$ in the demonstrations, and store all the tuples $[s_d, a_d, +1]$ in the replay buffer for HRN to obtain sufficient samples with "good action".

Both the HRN and the discriminator network will be used in the local cost function in Eq. (4) for providing learning signals to the policy and perform the update on it with TRPO. However, in this step, α is set to be a small value, so that we can update the discriminator network while learning the human reward network simultaneously with little effect on the cost function. That is to say, the human reward function has little effect on the policy learning with TRPO. Repeating the above steps until both the discriminator's expert accuracy and the generator accuracy reach 0.99, which can output a good, fixed cost function to effectively distinguish expert's state-action pairs from the agent's state-action pairs.

The second main step in GAIRL is the RL step, as shown in Algorithm 1 Part 2. By setting α to be a large value, the new cost function $c_{gairl}(s, a)$ consisting of both the cost function $c_{gail}(s, a)$ from the discriminator in GAIL and learned HRN will serve as a reward function for further RL method.

Algorithm 1 Part 2

```

15: while Policy Improves do
16:   Sample agent trajectories  $\tau_i$  from  $\pi_i$ 
17:   if Receive human feedback  $R_h$  with respect to  $[s, a]$ 
       from  $\tau_i$  then store  $[s, a, R_h]$  in  $\mathcal{B}_2$ 
18:     Randomly sample a batch of  $[s, a, R_h]$  from  $\mathcal{B}_2$ 
19:     Update  $\mathbb{H}$  using Rmsprop with loss  $\mathcal{L}_{hrn}$ 
20:   end if
21:   Update  $\pi_i$  using DQN/TD3 with reward
        $c_{gail}(s, a) = c_{gail}(s, a) + \alpha \mathbb{H}(s, a)$ 
22:    $i = i + 1$ 
23: end while

```

In addition, the human trainer can further provide evaluative feedback to train HRN. In this case, both the cost function $c_{gail}(s, a)$ learned from demonstrations and estimated HRN will provide rewards for the agent to perform updates on the policy. In our experiment, the value of α in the second main step varies in different tasks and will be experimentally optimized to achieve the best performance for a GAIRL agent. In our work, we choose DQN [47] for the RL step in tasks with continuous observation space and discrete action space and Twin Delayed Deep Deterministic policy gradient (TD3) [48] in tasks with continuous observation and continuous action space.

V. EXPERIMENTS

We tested our proposed method — GAIRL — in six physics-based control tasks, ranging from low-dimensional to high-dimensional tasks from the classic RL literature: Cart Pole, Mountain Car, Inverted Double Pendulum, Lunar Lander, Hopper and HalfCheetah. The Inverted Double Pendulum task is simulated with MuJoCo [49], Hopper and HalfCheetah are simulated with Pybullet [50], while other tasks are from OpenAI Gym [51]. Figure 1 shows screenshots of the six tasks.

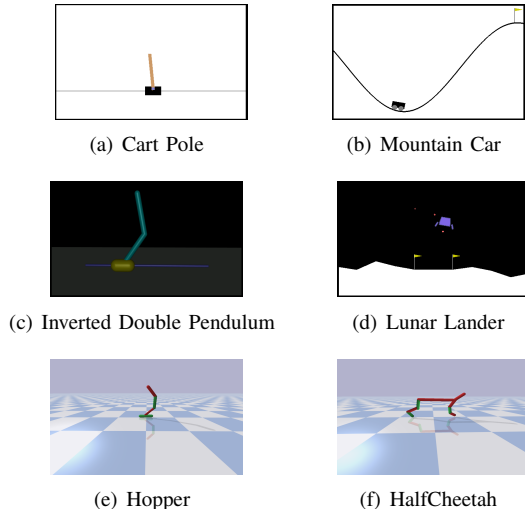


Fig. 1: Screenshots of the six tasks.

A. Experimental Tasks

Cart Pole: A pole is attached by an un-actuated joint to a cart, which moves along a frictionless track. The pole starts upright, and the goal is to prevent it from falling over by increasing and reducing the cart’s velocity. The state space is four-dimensional continuous and the action space is two-dimensional discrete. The reward is 1 for every step taken.

Mountain Car: A car started from the bottom of a valley and its goal is to climb to the top of the mountain. The state space is two-dimensional continuous and action space is three-dimensional discrete. The reward is given based on the vertical distance from the agent’s position to the bottom of a valley, and a custom reward function $|s[o] - (-0.06)|$ instead of the reward function defined in Gym is used.

Inverted Double Pendulum: This is a complex version of Cart Pole in 3D environment. The 2-link pendulum starts upright, and the goal is to prevent it from falling over by increasing and reducing the sliding block’s velocity. The state space is eleven-dimensional continuous and the action space is one-dimensional continuous. The reward is given at every step based on the angle of the pendulum at the end.

Lunar Lander: This is a simulation environment for testing and solving the rocket trajectory optimization — a classical optimal control problem. The state space is eight-dimensional continuous and the action space is four-dimensional discrete. The reward is given at every step based on the relative motion of the lander with respect to the landing pad.

Hopper&HalfCheetah: The goal of these tasks are to let the hopper and half part of a cheetah go forward as far as possible. In Hopper, the state space is fifteen-dimensional continuous and the action space is three-dimensional continuous. In HalfCheetah, the state space is 26-dimensional continuous and the action space is six-dimensional continuous. Reward is given at every step based on their relative motions with respect to the floor, control cost, etc.

Note that all these rewards mentioned above are only used for evaluating agents’ performance and generating demonstrations, but never for learning.

B. Experimental Setup

In each task, we train five agents: a GAIL agent as baseline; a GAIRL agent learning from rewards provided by the cost function $c_{gail}(s, a)$ extracted from demonstrations and human reward function learned during the GAIL alike step; a DQND or TD3D agent learning from the cost function $c_{gail}(s, a)$ extracted from expert demonstrations during the GAIL alike step; a DQNH or TD3H agent learning from human reward function learned during the GAIL alike step; a BC agent running imitation learning by behavioral cloning. For each task, a true reward function from OpenAI Gym [51] as described in Section V-A is used for evaluating the agent performance, but never for learning.

During experiments, we first generate demonstrated behavior for these tasks by running DQN/TD3 on these true reward functions to create demonstrated policies of different qualities — optimal or suboptimal, instead of using human experts to provide demonstrations. Then we sample datasets

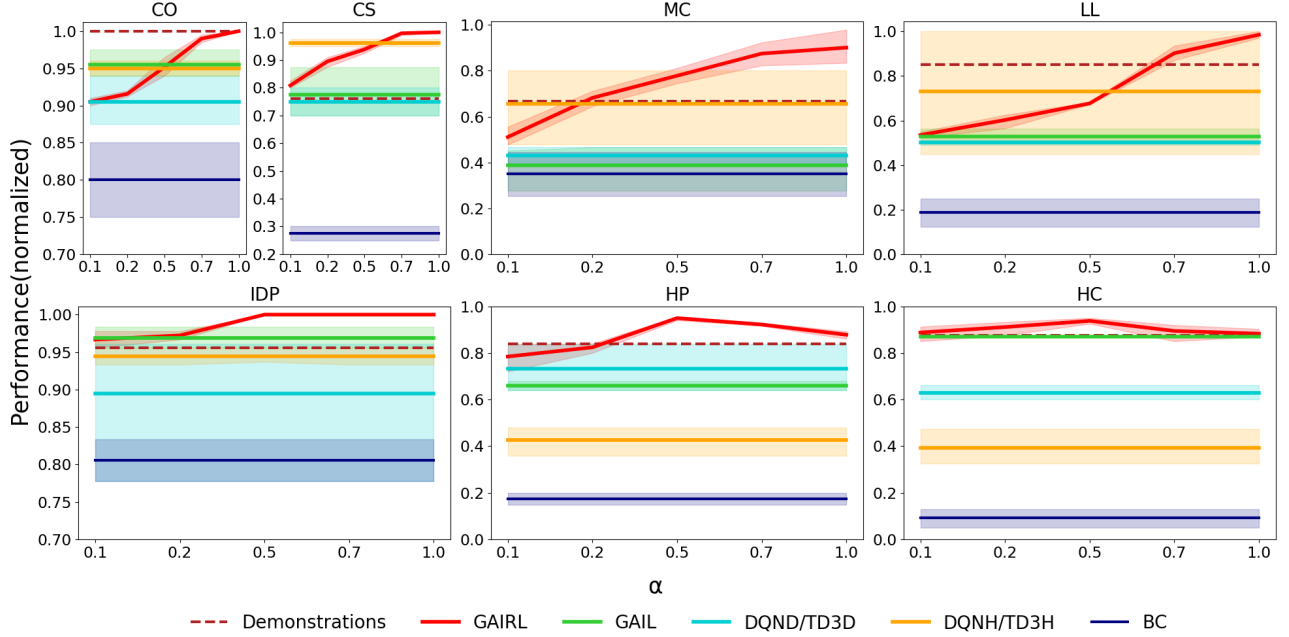


Fig. 2: Effect of the learned HRN on the final performance of the five agents. The y-axis is the normalized mean accumulated reward per 100 episodes with optimal performance as 1 in different tasks. The x-axis is α for balancing the cost function out of the discriminator in GAIL and HRN. Note: CO—Cart Pole with Optimal Demonstration, CS—Cart Pole with Suboptimal Demonstration, MC—Mountain Car, LL—Lunar Lander, IDP—Inverted Double Pendulum, HP—Hopper, HC—HalfCheetah.

of trajectories from the demonstrated policies, each consisting of about 200 state-action pairs. For all experiments, we use 10 demonstrations, as suggested by Ho et al. [22]. The first authors trained the human reward network HRN for all tasks. The weights of entropy term λ in our work is 10^{-3} .

We trained all agents’ policies of the same neural network architecture for all tasks: two hidden layers of 100 units each, with *tanh* nonlinearities in between. The architecture of discriminator network in GAIRL is the same as GAIL. The human reward network has two hidden layers of 100 units each, with *Relu* nonlinearities in between and *tanh* nonlinearities multiplying N in the output layer. All networks were always initialized randomly at the start of each trial. In each task, three random seeds are used for the environment simulator and the network initialization. Hopper and HalfCheetah tasks are run for 2 million timesteps, while the other tasks are run for 1 million timesteps. The performance metric, if not specified, used throughout the experiments is the mean accumulated reward per 100 episodes in terms of the true reward function from Gym.

VI. RESULTS AND DISCUSSION

In this section, we present and analyze the experimental results by comparing the performances of the five trained agents: GAIL agent, GAIRL agent, DQND/TD3D agent, DQNH/TD3H agent, BC agent. The shaded area is the 0.95 confidence interval and the bold line is the mean performance. Note that optimal performance and the performance of demonstrations with a confidence interval are also shown for reference. Both optimal and suboptimal demonstrations are offered in the Cart Pole task; only suboptimal demonstrations are offered in other tasks.

A. Effect of HRN on Agent’s Performance

We first analyze the effect of human evaluative feedback on agent’s learning by comparing the five agents’ final performance with varied α which is a weight vector for balancing the cost function $c_{gail}(s, a)$ out of the discriminator in GAIL and the learned HRN from human evaluative feedback, as in Eq. (4). Figure 2 shows the normalized final performance of the five agents in the six tasks. From Figure 2 we can see that, in relatively simple tasks (e.g., Cart Pole, Mountain Car, Lunar Lander), as α increases, the final performance of GAIRL agent goes up to optimal with optimal demonstrations and close to optimal even with suboptimal demonstrations. In Inverted Double Pendulum, Hopper and HalfCheetah, the final performance of GAIRL agent only improves and reaches close to optimal when α increases from 0.1 to 0.5, then stagnates in Inverted Double Pendulum and decreases in Hopper and HalfCheetah. Our results show that with a proper value of α in all tasks, the GAIRL agent can learn much better than learning from demonstrations (GAIL, DQND/TD3D, BC) and human evaluative feedback (DQNH/TD3H) alone separately, achieving optimal or close to optimal performance.

B. Learning Curve

We further analyze the effect of human evaluative feedback on GAIRL agent’s performance in the learning process by comparing the learning curves of the four trained agents: GAIL agent, GAIRL agent, DQND/TD3D agent, DQNH/TD3H agent. BC agent is not shown because it does not learn interactively. Note that α is set to be able to achieve the best performance in all tasks (1 for Cart Pole, Mountain Car and Lunar Lander, 0.5 for Inverted Double Pendulum, Hopper and HalfCheetah).

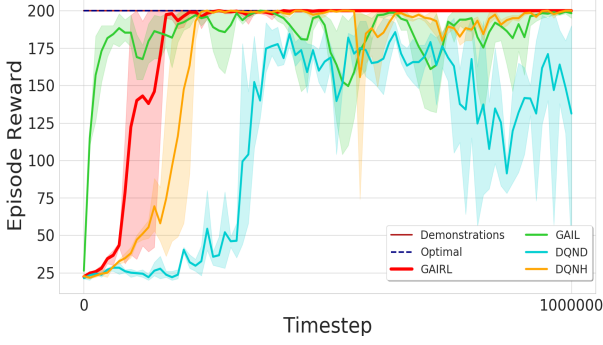


Fig. 3: The four agents’ learning curves with optimal demonstrations in Cart Pole.

1) *Low-dimensional Tasks:* Figure 3 shows four agents’ learning curves with optimal demonstrations in Cart Pole. From Figure 3 we can see that, with optimal demonstrations, the performance of GAIL agent almost immediately reaches the first peak which is faster but worse than the GAIRL agent. However, the performance of the GAIRL agent in the first peak is already close to optimal and stabilizes shortly after that, while the performance of GAIL agent still fluctuates below the optimal performance with an unstable policy reaching the optimal performance occasionally. Both DQND and DQNH agents learn slower than the GAIL and GAIRL agent. The performance of the DQND agent fluctuates in a similar way as the GAIL agent, while the DQNH agent learns faster than the DQND agent and reaches the optimal performance after final training.

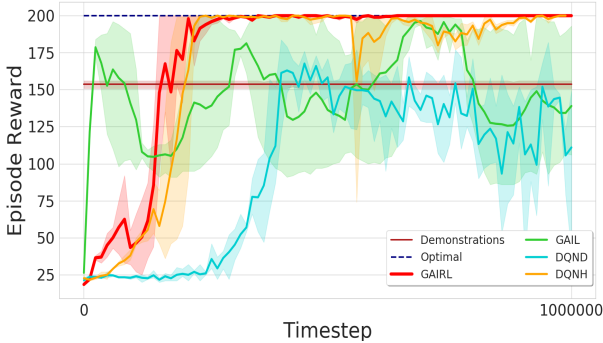


Fig. 4: The four agents’ learning curves with suboptimal demonstrations in Cart Pole.

Figure 4 shows four agents’ learning curves with suboptimal demonstrations in Cart Pole. As shown in Figure 4, even with suboptimal demonstrations, the performance of the GAIRL agent still reaches the optimal performance in the first peak and stabilizes afterwards, while the GAIL agent’s performance fluctuates dramatically around the performance of demonstrations with a faster learning speed. Same to results in Figure 3, while still learning slower, the performance of the DQND agent fluctuates around the performance of demonstrations and the DQNH agent learns much faster and obtains a stable optimal policy finally.

The four agents’ learning with suboptimal demonstrations

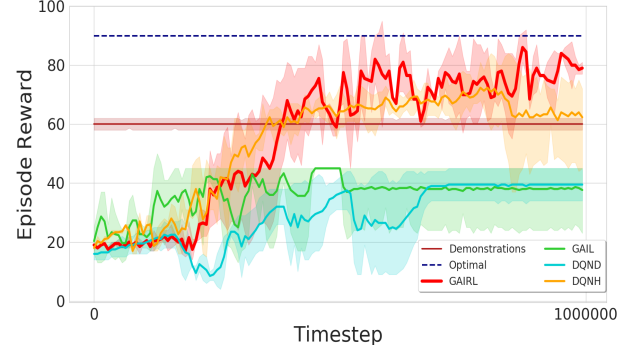


Fig. 5: The four agents’ learning curves with suboptimal demonstrations in Mountain Car.

were also tested in Mountain Car, as shown in Figure 5. From Figure 5 we can see that, similar to Figure 4, even with far from optimal demonstrations, the performance of the GAIRL agent can still surpass the demonstrations and be close to the optimal one. In contrast, although learning faster, the performance of the GAIL agent is far from the performance of demonstrations. The DQND agent still learns much slower than the GAIL and GAIRL agent, reaching a similar performance to the GAIL agent finally. However, the DQNH agent learns much faster and its final performance is better than the demonstrations but worse than the GAIRL agent.

2) *High-dimensional Tasks:* We also tested and compared the performances of the four agents with suboptimal demonstrations in four high-dimensional tasks: Inverted Double Pendulum, Lunar Lander, Hopper and HalfCheetah.

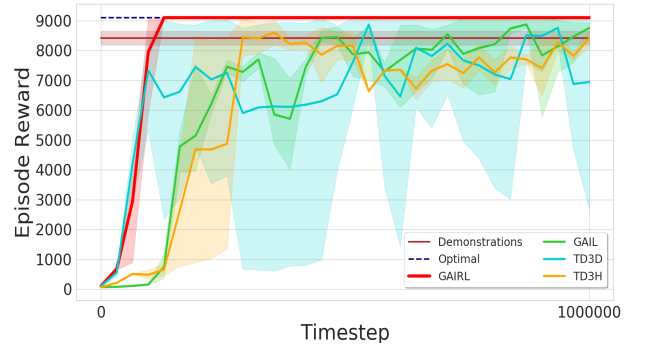


Fig. 6: The four agents’ learning curves with suboptimal demonstrations in Inverted Double Pendulum.

Figure 6 shows four agents’ learning curves in Inverted Double Pendulum. Different from results in the low-dimensional tasks, Figure 6 shows both GAIRL and TD3D agents learn much faster than the GAIL agent, which might be because of the superiority of TD3 used in GAIRL. The GAIRL agent achieves an optimal performance in the first peak and stabilizes immediately after that, while the performance of GAIL, TD3D and TD3H agents fluctuate around the performance of demonstrations.

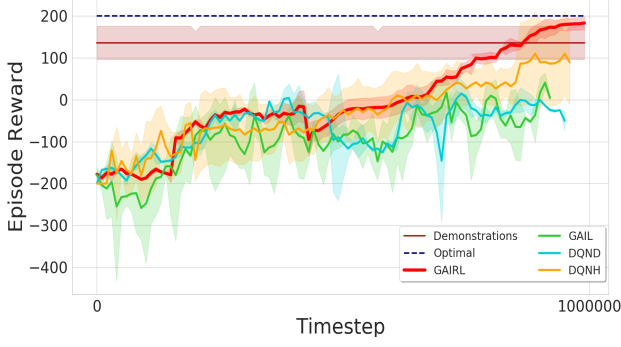


Fig. 7: The four agents’ learning curves with suboptimal demonstrations in Lunar Lander.

Figure 7 shows four agents’ learning curves in Lunar Lander. Different from the Inverted Double Pendulum task, the performance of demonstrations used here is less stable with a relatively high variance. From Figure 7 we can see that, while both the GAIL and DQND agents learn slowly at the beginning, deteriorate in the middle of training and reach a performance far worse than demonstrations, the GAIRL agent reaches a close to optimal performance after a long training time finally. The DQNH agent’s learning is quite similar to that of the GAIRL agent, with a final performance worse than the demonstrations but better than those of the GAIL and DQND agents.

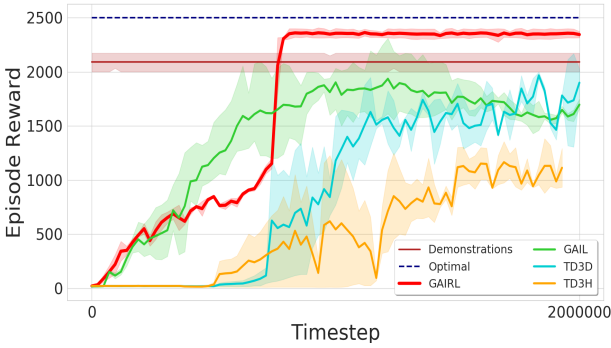


Fig. 8: The four agents’ learning curves with suboptimal demonstrations in Hopper.

Figure 8 shows four agents’ learning curves in Hopper. From Figure 8 we can see that, the GAIL agent learns a bit faster than the GAIRL agent but with a final performance worse than the demonstrations, while the GAIRL agent achieves a performance much better than the demonstrations in the first peak after a third of the training time and stabilizes after that. Both TD3D and TD3H agents learn much slower than the GAIL and GAIRL agents, while the final performance of the TD3D agent is similar to that of GAIL agent and the TD3H agent achieves a far worse performance.

Figure 9 shows four agents’ learning curves in HalfCheetah. Different from other tasks, all four agents learn fast in HalfCheetah with the speed of the TD3D agent a bit faster than the other three agents. However, both performances of

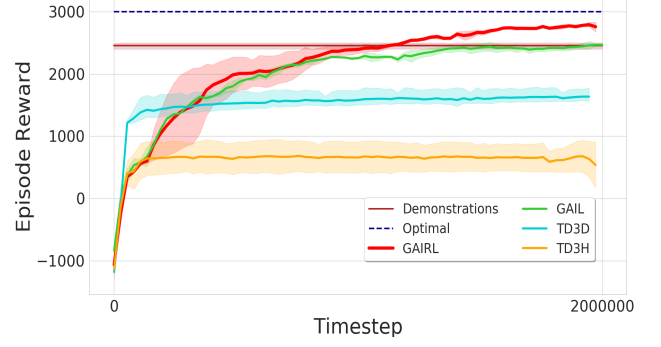


Fig. 9: The four agents’ learning curves with suboptimal demonstrations in HalfCheetah.

the TD3H agent and TD3D agent stabilize after reaching the first peak and are far worse than the performance of demonstrations. In contrast, both performances of the GAIL agent and GAIRL agent rise steadily in a similar way. The GAIRL agent’s final performance is close to optimal and better than that of demonstrations, while the GAIL agent reaches a final performance almost the same as that of demonstrations.

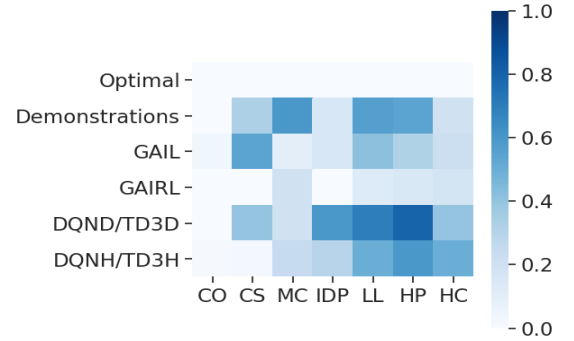


Fig. 10: Variance of the four agents’ final policies compared to the expert and optimal policy in the six tasks. Note: CO—Cart Pole with Optimal Demonstration, CS—Cart Pole with Suboptimal Demonstration, MC—Mountain Car, IDP—Inverted Double Pendulum, LL—Lunar Lander, HP—Hopper, HC—HalfCheetah.

3) *Stability Analysis:* We also studied the stability of the final learned policy of the four agents by testing them for 10 times in each task and computing the variance over the 10 performances for each policy. The variances of all policies, including the demonstrated policy and the optimal policy, are shown in Figure 10. The optimal policy is always stable while the stability of the demonstrated policy is different in each task. Figure 10 shows that the GAIRL agent always learns a much more stable policy than the demonstrated policy and most of the time almost as stable as the optimal one, while the GAIL agent’s policy is only slightly more stable than the demonstrated policy and even a bit less stable in Cart Pole with both optimal and suboptimal demonstrations. In addition, the policy of DQND/TD3D and DQNH/TD3H agents become generally less stable as the task’s difficulty

increases (from left to right in Figure 10), while the stability of the GAIRL agent keeps at a similar and much higher level than both of them. This suggests the demonstrations and human evaluative feedback might have a complementary effect. Demonstrations provide a high-level initialization of the human’s overall reward function, while human evaluative feedback like preferences can explore specific, fine-grained aspects of it [52].

In summary, our results suggest that for both low-dimensional and high-dimensional tasks with both optimal and suboptimal demonstrations, a GAIRL agent can learn a more stable policy with optimal or close to optimal performance, while the performance of the GAIL agent is upper bounded by the performance of demonstrations or even worse than it. In addition, our results indicate the superiority of GAIRL over GAIL might be because of the complementary effect of the demonstrations and human evaluative feedback.

VII. CONCLUSION

In this paper, to address the limit of GAIL that it seldom surpasses the performance of demonstrations, we propose a model-free framework — GAN-Based Interactive Reinforcement Learning (GAIRL) by combining the advantages of GAIL and interactive RL from human evaluative feedback. We tested GAIRL in six physics-based control tasks from the classic RL literature. Our results suggest that with both optimal and suboptimal demonstrations, the GAIRL agent can learn a more stable policy with optimal or close to optimal performance, while the performance of the GAIL agent is upper bounded by the the performance of demonstrations or even worse than it. In addition, our results indicate the superiority of GAIRL over GAIL might be because human evaluative feedback is complementary to demonstrations.

REFERENCES

- [1] R. Sutton and A. Barto, *Reinforcement learning: an introduction*. MIT Press, 1998.
- [2] J. Kober, J. A. Bagnell, and J. Peters, “Reinforcement learning in robotics: A survey,” *The International Journal of Robotics Research*, vol. 32, no. 11, pp. 1238–1274, 2013.
- [3] V. Mnih, K. Kavukcuoglu, D. Silver, A. A. Rusu, J. Veness, M. G. Bellemare, A. Graves, M. Riedmiller, A. K. Fidjeland, G. Ostrovski, et al., “Human-level control through deep reinforcement learning,” *Nature*, vol. 518, no. 7540, pp. 529–533, 2015.
- [4] G. A. DeepMind, “Mastering the real-time strategy game starcraft ii,” 2019.
- [5] D. Silver, J. Schrittwieser, K. Simonyan, I. Antonoglou, A. Huang, A. Guez, T. Hubert, L. Baker, M. Lai, A. Bolton, et al., “Mastering the game of go without human knowledge,” *Nature*, vol. 550, no. 7676, pp. 354–359, 2017.
- [6] N. Heess, D. TB, S. Sriram, J. Lemmon, J. Merel, G. Wayne, Y. Tassa, T. Erez, Z. Wang, S. Eslami, et al., “Emergence of locomotion behaviours in rich environments,” *arXiv preprint arXiv:1707.02286*, 2017.
- [7] C. Florensa, Y. Duan, and P. Abbeel, “Stochastic neural networks for hierarchical reinforcement learning,” in *Proceedings of International Conference on Learning Representations (ICLR)*, 2017.
- [8] O. M. Andrychowicz, B. Baker, M. Chociej, R. Jozefowicz, B. McGrew, J. Pachocki, A. Petron, M. Plappert, G. Powell, A. Ray, et al., “Learning dexterous in-hand manipulation,” *The International Journal of Robotics Research*, vol. 39, no. 1, pp. 3–20, 2020.
- [9] V. G. Goecks, G. M. Gremillion, V. J. Lawhern, J. Valasek, and N. R. Waytowich, “Integrating behavior cloning and reinforcement learning for improved performance in dense and sparse reward environments,” in *Proceedings of the 19th International Conference on Autonomous Agents and MultiAgent Systems (AAMAS)*, 2020, pp. 465–473.
- [10] M. Riedmiller, R. Hafner, T. Lampe, M. Neunert, J. Degraeve, T. Wiele, V. Mnih, N. Heess, and J. T. Springenberg, “Learning by playing solving sparse reward tasks from scratch,” in *Proceedings of International Conference on Machine Learning (ICML)*. PMLR, 2018, pp. 4344–4353.
- [11] G. Li, B. He, R. Gomez, and K. Nakamura, “Interactive reinforcement learning from demonstration and human evaluative feedback,” in *Proceedings of the 27th IEEE International Symposium on Robot and Human Interactive Communication (RO-MAN)*. IEEE, 2018, pp. 1156–1162.
- [12] S. Ross and D. Bagnell, “Efficient reductions for imitation learning,” in *Proceedings of the 30th International Conference on Artificial Intelligence and Statistics*, 2010, pp. 661–668.
- [13] A. Y. Ng, S. J. Russell, et al., “Algorithms for inverse reinforcement learning,” in *Proceedings of International Conference on Machine Learning (ICML)*, vol. 1, 2000, p. 2.
- [14] P. Abbeel and A. Y. Ng, “Apprenticeship learning via inverse reinforcement learning,” in *Proceedings of the 21st International Conference on Machine Learning (ICML)*, 2004, p. 1.
- [15] U. Syed, M. Bowling, and R. E. Schapire, “Apprenticeship learning using linear programming,” in *Proceedings of the 25th International Conference on Machine Learning (ICML)*, 2008, pp. 1032–1039.
- [16] U. Syed and R. E. Schapire, “A game-theoretic approach to apprenticeship learning,” in *Advances in Neural Information Processing Systems (NIPS)*, 2008, pp. 1449–1456.
- [17] B. D. Ziebart, A. L. Maas, J. A. Bagnell, and A. K. Dey, “Maximum entropy inverse reinforcement learning,” in *Proceedings of the AAAI Conference on Artificial Intelligence*, vol. 8. Chicago, IL, USA, 2008, pp. 1433–1438.
- [18] M. Bloem and N. Bambos, “Infinite time horizon maximum causal entropy inverse reinforcement learning,” in *Proceedings of the 53rd IEEE Conference on Decision and Control*. IEEE, 2014, pp. 4911–4916.
- [19] A. Rajeswaran, V. Kumar, A. Gupta, G. Vezzani, J. Schulman, E. Todorov, and S. Levine, “Learning complex dexterous manipulation with deep reinforcement learning and demonstrations,” in *Proceedings of Robotics: Science and Systems (RSS)*, 2018.
- [20] A. Nagabandi, G. Kahn, R. S. Fearing, and S. Levine, “Neural network dynamics for model-based deep reinforcement learning with model-free fine-tuning,” in *Proceedings of IEEE International Conference on Robotics and Automation (ICRA)*. IEEE, 2018, pp. 7559–7566.
- [21] J. Ho, J. Gupta, and S. Ermon, “Model-free imitation learning with policy optimization,” in *Proceedings of International Conference on Machine Learning (ICML)*, 2016, pp. 2760–2769.
- [22] J. Ho and S. Ermon, “Generative adversarial imitation learning,” in *Advances in Neural Information Processing Systems (NIPS)*, 2016, pp. 4565–4573.
- [23] S. Ermon, Y. Xue, R. Toth, B. Dilkina, R. Bernstein, T. Damoulas, P. E. Clark, S. DeGloria, A. Mude, C. Barrett, et al., “Learning large-scale dynamic discrete choice models of spatio-temporal preferences with application to migratory pastoralism in east africa,” in *Proceedings of the AAAI Conference on Artificial Intelligence*, 2015, pp. 644–650.
- [24] I. Goodfellow, J. Pouget-Abadie, M. Mirza, B. Xu, D. Warde-Farley, S. Ozair, A. Courville, and Y. Bengio, “Generative adversarial nets,” in *Advances in Neural Information Processing Systems (NIPS)*, 2014, pp. 2672–2680.
- [25] X. B. Peng, A. Kanazawa, S. Toyer, P. Abbeel, and S. Levine, “Variational discriminator bottleneck: Improving imitation learning, inverse rl, and gans by constraining information flow,” in *Proceedings of International Conference on Learning Representations (ICLR)*, 2018.
- [26] X. B. Peng, P. Abbeel, S. Levine, and M. van de Panne, “Deepmimic: Example-guided deep reinforcement learning of physics-based character skills,” *ACM Transactions on Graphics (TOG)*, vol. 37, no. 4, pp. 1–14, 2018.
- [27] G. Warnell, N. Waytowich, V. Lawhern, and P. Stone, “Deep tamer: Interactive agent shaping in high-dimensional state spaces,” in *Proceedings of the 32nd AAAI Conference on Artificial Intelligence*, 2018.
- [28] A. Y. Ng, D. Harada, and S. Russell, “Policy invariance under reward transformations: Theory and application to reward shaping,” in *Proceedings of International Conference on Machine Learning (ICML)*, vol. 99, 1999, pp. 278–287.
- [29] G. Li, R. Gomez, K. Nakamura, and B. He, “Human-centered reinforcement learning: a survey,” *IEEE Transactions on Human-Machine Systems*, vol. 49, no. 4, pp. 337–349, 2019.
- [30] E. T. Jaynes, “Information theory and statistical mechanics,” *Physical Review*, vol. 106, no. 4, p. 620, 1957.

- [31] N. D. Ratliff, D. Silver, and J. A. Bagnell, "Learning to search: Functional gradient techniques for imitation learning," *Autonomous Robots*, vol. 27, no. 1, pp. 25–53, 2009.
- [32] B. C. Stadie, P. Abbeel, and I. Sutskever, "Third-person imitation learning," *arXiv preprint arXiv:1703.01703*, 2017.
- [33] F. Torabi, G. Warnell, and P. Stone, "Generative adversarial imitation from observation," *arXiv preprint arXiv:1807.06158*, 2018.
- [34] M. Arjovsky and L. Bottou, "Towards principled methods for training generative adversarial networks," in *Proceedings of International Conference on Learning Representations (ICLR)*, 2017.
- [35] Z. Wang, J. Merel, S. Reed, G. Wayne, N. de Freitas, and N. Heess, "Robust imitation of diverse behaviors," in *Proceedings of the 31st International Conference on Neural Information Processing Systems (NIPS)*, 2017, pp. 5326–5335.
- [36] T. Hester, M. Vecerik, O. Pietquin, M. Lanctot, T. Schaul, B. Piot, D. Horgan, J. Quan, A. Sendonaris, I. Osband, et al., "Deep q-learning from demonstrations," in *Proceedings of the AAAI Conference on Artificial Intelligence*, vol. 32, no. 1, 2018.
- [37] Y. Gao, H. Xu, J. Lin, F. Yu, S. Levine, and T. Darrell, "Reinforcement learning from imperfect demonstrations," in *Proceedings of International Conference on Learning Representations (ICLR) Workshop*, 2018.
- [38] S. Reddy, A. D. Dragan, and S. Levine, "Sqil: Imitation learning via reinforcement learning with sparse rewards," in *Proceedings of International Conference on Learning Representations (ICLR)*, 2019.
- [39] M. Jing, X. Ma, W. Huang, F. Sun, C. Yang, B. Fang, and H. Liu, "Reinforcement learning from imperfect demonstrations under soft expert guidance," in *Proceedings of the AAAI Conference on Artificial Intelligence*, vol. 34, no. 04, 2020, pp. 5109–5116.
- [40] A. L. Thomaz and C. Breazeal, "Teachable robots: Understanding human teaching behavior to build more effective robot learners," *Artificial Intelligence*, vol. 172, no. 6-7, pp. 716–737, 2008.
- [41] C. J. Watkins and P. Dayan, "Q-learning," *Machine Learning*, vol. 8, no. 3-4, pp. 279–292, 1992.
- [42] W. B. Knox and P. Stone, "Interactively shaping agents via human reinforcement: The TAMER framework," in *Proceedings of the 5th International Conference on Knowledge Capture*, 2009, pp. 9–16.
- [43] R. Loftin, B. Peng, J. MacGlashan, M. L. Littman, M. E. Taylor, J. Huang, and D. L. Roberts, "Learning behaviors via human-delivered discrete feedback: modeling implicit feedback strategies to speed up learning," *Autonomous Agents and Multi-agent Systems*, vol. 30, no. 1, pp. 30–59, 2016.
- [44] J. MacGlashan, M. K. Ho, R. Loftin, B. Peng, G. Wang, D. L. Roberts, M. E. Taylor, and M. L. Littman, "Interactive learning from policy-dependent human feedback," in *Proceedings of International Conference on Machine Learning (ICML)*. PMLR, 2017, pp. 2285–2294.
- [45] D. Arumugam, J. K. Lee, S. Saskin, and M. L. Littman, "Deep reinforcement learning from policy-dependent human feedback," *arXiv preprint arXiv:1902.04257*, 2019.
- [46] J. Schulman, S. Levine, P. Abbeel, M. Jordan, and P. Moritz, "Trust region policy optimization," in *Proceedings of International Conference on Machine Learning (ICML)*, 2015, pp. 1889–1897.
- [47] V. Mnih, K. Kavukcuoglu, D. Silver, A. Graves, I. Antonoglou, D. Wierstra, and M. Riedmiller, "Playing atari with deep reinforcement learning," in *Proceedings of Deep Learning Workshop at International Conference on Neural Information Processing Systems (NIPS)*, 2013.
- [48] S. Fujimoto, H. Hoof, and D. Meger, "Addressing function approximation error in actor-critic methods," in *Proceedings of International Conference on Machine Learning (ICML)*. PMLR, 2018, pp. 1587–1596.
- [49] E. Todorov, T. Erez, and Y. Tassa, "Mujoco: A physics engine for model-based control," in *Proceedings of IEEE/RSJ International Conference on Intelligent Robots and Systems (IROS)*. IEEE, 2012, pp. 5026–5033.
- [50] E. Coumans and Y. Bai, "Pybullet, a python module for physics simulation for games, robotics and machine learning," 2016.
- [51] G. Brockman, V. Cheung, L. Pettersson, J. Schneider, J. Schulman, J. Tang, and W. Zaremba, "Openai gym," *arXiv preprint arXiv:1606.01540*, 2016.
- [52] E. Btyik, D. P. Losey, M. Palan, N. C. Landolfi, G. Shevchuk, and D. Sadigh, "Learning reward functions from diverse sources of human feedback: Optimally integrating demonstrations and preferences," *arXiv preprint arXiv:2006.14091*, 2020.



Jie Huang received a Bachelor degree in electronic information science and technology from School of Information Science and Engineering, Ocean University of China in 2019. He is currently pursuing the master's degree with the School of Information Science and Engineering, Ocean University of China, Qingdao, China. His current research interests include reinforcement learning, human agent/robot interaction, imitation learning and robotics.



Rongshun Juan received a Bachelor degree in electronic information science and technology from School of Information Science and Engineering, Ocean University of China in 2019. He is currently pursuing the master's degree with the School of Information Science and Engineering, Ocean University of China, Qingdao, China. His current research interests include reinforcement learning, human agent/robot interaction, transfer learning and robotics.



tion, multimodal interaction and robotics.

Randy Gomez received M.Eng.Sci. in Electrical Engineering at the University of New South Wales (UNSW), Australia in 2002. He obtained his Ph.D. in 2006 from the Graduate School of Information Science, Nara Institute of Science and Technology, Japan. He was a researcher at Kyoto University until 2012 under the auspices of the Japan Society for the Promotion of Science (JSPS) research fellowship. Currently, he is a senior scientist at Honda Research Institute Japan. His research interests include robust speech recognition, acoustic modeling and adaptation.



research interests are in the field of robotics, control systems, and signal processing. He is currently a member of IEEE.

Keisuke Nakamura received a B.E. in 2007 from the Department of Control and System Engineering, Tokyo Institute of Technology, Japan. He also studied in the Department of Electronic and Electrical Engineering at the University of Strathclyde, United Kingdom from 2007 to 2008. He received an M.E. from the Department of Mechanical and Control Engineering at Tokyo Institute of Technology in 2010, and Ph.D. in Informatics in 2013 from Kyoto University, Japan. He is currently a senior scientist for Honda Research Institute Japan, Co., Ltd. His



software system in underwater vehicle.

Qixin Sha received the B.S. degree in communication engineering from Ocean University of China in 2007, and the M.S. degree in communication and information systems from Ocean University of China in 2010. He worked at Qingdao Bailing Technology Co., Ltd. and Alcatel-Lucent Qingdao R & D Center from 2010 to 2014 as a software engineer. He is currently working as an experimenter in the Department of Electronic Engineering, Ocean University of China. His research interests include the design and development of architecture, decision-making and



Bo He received a PhD degree from Harbin Institute of Technology in 1999. He was a researcher in Nanyang Technological University from 2000 to 2002. He is currently a full professor in Ocean University of China. His research interests include SLAM, machine learning and robotics. He is currently a member of IEEE.



Guangliang Li received a Bachelor and M.Sc. degree from School of Control Science and Engineering in Shandong University in 2008 and 2011 respectively. In 2016, he received a Ph.D. degree in Computer Science from the University of Amsterdam, The Netherlands. He was a visiting researcher in Delft University of Technology, The Netherlands, and a research intern in Honda Research Institute Japan, Co., Ltd. Japan. He is currently a lecturer at Ocean University of China. His research interests include reinforcement learning, human agent/robot interaction and robotics. He is a member of IEEE.